Effect of Cations on the Structure of Bilayers Formed by Lipopolysaccharides Isolated from *Pseudomonas aeruginosa* PAO1

Norbert Kučerka,*,†,‡ Erzsebet Papp-Szabo,§,||,⊥ Mu-Ping Nieh,† Thad A. Harroun,# Sarah R. Schooling,§,||,⊥ Jeremy Pencer,▽ Eric A. Nicholson,† Terry J. Beveridge,§,||,⊥ and John Katsaras*,†,||,⊥,#,○

Canadian Neutron Beam Centre, National Research Council, Chalk River, Ontario K0J 1J0, Canada, Department of Physical Chemistry of Drugs, Faculty of Pharmacy, Comenius University, 83232 Bratislava, Slovakia, Department of Molecular and Cellular Biology, Biophysics Interdepartmental Group, Advanced Food and Materials Network, Networks of Centres of Excellence, University of Guelph, Guelph, Ontario N1G 2W1, Canada, Department of Physics, Brock University, 500 Glenridge Avenue, St. Catharines, Ontario L2S 3A1, Canada, Atomic Energy of Canada Limited, Chalk River Laboratories, Chalk River, Ontario K0J 1J0, Canada, and Guelph−Waterloo Physics Institute, University of Guelph, Guelph, Ontario N1G 2W1, Canada

Received: January 28, 2008

The asymmetric outer membrane of Gram-negative bacteria contains lipopolysaccharides (LPSs) which contribute significantly to the bacterium's surface properties and play a crucial role in regulating membrane permeability. We report on neutron diffraction studies performed on aligned, self-assembled bilayers of Na-, Ca-, and Mg-salt forms of LPS isolated from *Pseudomonas aeruginosa* PAO1. From the one-dimensional neutron scattering length density profiles we find that water penetrates Ca^{2+}-LPS bilayers to a lesser extent than either Na^{+}- or Mg^{2+}-LPS bilayers. This differential water penetration could have implications as to how small molecules permeate the outer membrane of Gram-negative bacteria and, possibly, how nonlamellar phases are formed.

Introduction

Bacterial lipopolysaccharides (LPSs) are the major lipid component making up the outermost leaflet of the asymmetric outer membrane (OM) of Gram-negative bacteria.[1,2] LPS contributes to the OM's structural integrity and also protects the bacteria from a variety of toxic molecules, such as certain antibiotics (e.g., penicillin), digestive enzymes (e.g., lysozyme), detergents, heavy metals, bile salts, and some dyes. On the other hand, the OM's inner leaflet is predominantly composed of common lipids such as phosphatidyl-ethanolamine (PE), phosphatidylcholine (PC), phosphatidylglycerol (PG), and cardiolipin (diphosphatidylglycerol).[3] The passage of nucleotides, disaccharides, amino acids, vitamins, and iron for nutritional growth are usually transported through the OM by porin proteins, but it is LPS that provides the bacteria with its remarkable selectively permeable membrane that is resistant to a variety of deleterious agents. In particular, *Pseudomonas aeruginosa* is well-noted for its recalcitrance to conventional antibiotic therapy, partly as a result of its unique surface chemistry.[4] For this reason, and also due to the ubiquity of *P. aeruginosa* and its impact upon health as both an opportunistic and nosocomial pathogen, this organism represents an attractive candidate for study.

Although LPS molecules are structurally diverse, they share a common architecture comprised of three basic units (Figure 1). The first is a lipid A moiety which anchors the LPS molecule into the hydrophobic domain of the OM. It consists of two phosphorylated glucosamine units that are typically acylated with four to six fatty acids and is considered to be responsible for most of the toxicity associated with LPS. Second, the LPS's core oligosaccharide is made up of 8−12 monosaccharide units and is connected to lipid A by 2-keto-3-deoxyoctonoic acid (Kdo). Finally, the third part is formed by repetitive monosaccharide subunits (i.e., O-side chain), which are responsible for much of the bacterium's immunospecificity.[5]

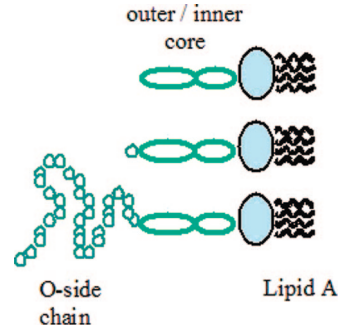

Figure 1. Schematic of LPS architectures. LPSs consist of a hydrophobic region formed by lipid A, and an extensive hydrophilic region made up of the inner and outer cores, with additional O-side specific chains. (a) "Rough" LPS does not contain O-side chains. (b) "Semirough" LPS has an O-side chain with only one repeat unit. (c) "Smooth" LPS with an O-side chain made up of up to 50 trisaccharide repeat units.

LPS imparts three important characteristics to Gram-negative bacteria. The O-polysaccharide chains function as antigens and are used by clinical microbiologists to distinguish different species of the bacteria by a simple agglutination assay. Lipid

* Corresponding authors. E-mail: Norbert.Kucerka@nrc-cnrc.gc.ca (N.K.), John.Katsaras@nrc-cnrc.gc.ca (J.K.).
† National Research Council.
‡ Comenius University.
§ Department of Molecular and Cellular Biology, University of Guelph.
|| Biophysics Interdepartmental Group, University of Guelph.
⊥ Advanced Food and Materials Network, University of Guelph.
Brock University.
▽ Atomic Energy of Canada Limited.
○ Guelph−Waterloo Physics Institute, University of Guelph.

10.1021/jp8027963 CCC: $40.75
Published on Web 06/13/2008

A is a pyrogenic endotoxin, which when released by lysis, either by antibiotics or phagocyte ingestion, promotes the release of interleukin, stimulating the hypothalamus and inducing fever. More seriously, less than one-millionth of a milligram of endotoxin released during septicemia is required to cause septic shock, resulting in a precipitous drop in blood pressure. Finally, disease pathogenesis requires bacterial colonization, which fundamentally requires cell adhesion to some tissue surface within the host. In addition to the roles of other macromolecules (e.g., fimbriae and pili[6]) in cell adhesion, its properties can also be modified by LPS's O-chains.

The structural diversity of O-antigens across species is remarkable; over 60 monosaccharides and 30 different noncarbohydrate components have been recognized.[7] Given the variety of possible LPS types available, we have focused on smooth LPS isolates from *P. aeruginosa*. *Pseudomonas* species are found in water, soil, and on most food plant types, such as fruits and vegetables. *P. aeruginosa*, in particular, demonstrates a high adaptability to thrive in a wide variety of aqueous solutions, including disinfectants and soaps, making it problematic in hospital settings. Also, a number of virulence factors are associated with *P. aeruginosa*, contributing to its ability to cause different infections, including "swimmer's ear", contaminated contact lenses, septicemia from contaminated intravenous needles, and peculiarly, infections to the lungs of cystic fibrosis patients.[8,9]

P. aeruginosa produces two different O-chain species, commonly known as A-band and B-band polysaccharides. Its antigenic specificity is determined by B-band polysaccharides, whereas A-band polysaccharides are antigenically conserved across the *Pseudomonas* species. The diversity of B-band saccharides on the surface of *P. aeruginosa* has a major influence on antibiotic binding and antibiotic-induced killing.[10] In addition, it has been demonstrated that the O-antigen chemistry is vital for other surface-associated activities, such as interactions with metals and nanomineral formation,[11] surface adhesion and colonization, the ability to cause infection and disease, as well as biofilm formation.[4]

Besides LPS chemical diversity, the substantial differences in the size of LPS molecules are also typical of *P. aeruginosa*. O-side specific chains may be expressed as "smooth" forms containing up to 50 repeating units,[12] whereas a large portion of LPS molecules are in the "rough" (i.e., no O-chain) or "semirough" form (i.e., with one O-chain repeat unit of B-band polysaccharide attached to the core). Moreover, depending on ambient conditions, rough LPS mutants have exhibited diverse structural polymorphism,[13] most likely also present in smooth mutants.[14] Although most biological activity has been associated with lipid A, there are considerable differences in the infections reported between smooth and rough phenotypes.[15]

The unique chemistry and structure of LPS is believed to contribute to specific LPS−LPS interactions, which can be modulated by cations like Na^+, Ca^{2+} and Mg^{2+}. These cations are thought to play an important role in LPS organization by bridging the proximal, negatively charged functional groups, thereby overcoming the strong electrostatic repulsions present between LPS molecules.[16,17] Although a complete understanding of the physicochemical roles of these metallic cations is yet to be established, experiments have reported of structural changes to the OM in response to different salt conditions.[18–20] Perhaps the most important consequence of these structural changes is the change in the physicochemical properties and biological activity as measured by the ability of LPS to induce cytokine release from human peripheral blood mononuclear cells.[20] Natural salt isolates of rough LPS from *Salmonella minnesota* (which usually include Na^+ and K^+ cations) are measurably more active than those with Mg^{2+} cation, and orders of magnitude more active than with Ca^{2+}.

Differences in the biological activity of LPS have been correlated with increased order of the lipid A acyl chains, accompanied by the formation of multilamellar bilayers—which have typically been determined to be biologically inactive—rather than cubic or unilamellar aggregates.[21] When discussing the heterogeneity of LPS types, a crucial parameter dictating such complex reorganization is likely the shape of the LPS itself. For a single LPS type, the crucial parameter may be the degree of hydration. For example, we have recently reported of the disappearance of lamellar reflections when liquid-crystalline LPS multibilayers were subjected to high levels of hydration.[14] More importantly, we observed water molecules penetrating deep into LPS bilayers, including the bilayer center. We hypothesized that this penetration increases up to a critical point, beyond which the multibilayer assembly is destroyed. Such a mechanism for bilayer destabilization could provide a general explanation of how nonlamellar phases are formed and how small molecules penetrate the OM of Gram-negative bacteria.

Here we report on the effects of three different cations (i.e., Na^+, Ca^{2+}, Mg^{2+}) on the multilamellar structure of bilayers formed using LPS isolated from *P. aeruginosa* PAO1. From the difference one-dimensional neutron scattering length density (1D SLD) profiles, we find lower penetration of water molecules through Ca^{2+}-LPS bilayers, when compared to Na^+- or Mg^{2+}-LPS bilayers.

Experimental Procedures

LPS Isolation and Salt Form Conversion. Cultures of *P. aeruginosa* PAO1 (serotype 05) were grown to an early stationary phase in trypticase soy broth (BBL; 37 °C, 125 rpm), and LPS was isolated using the protocol described by Darveau and Hancock.[22] This method uses high EDTA (ethylenediaminetetraacetic acid) concentrations and involves two precipitation steps with two volumes of 0.375 M $MgCl_2$ in 95% ethanol, with a final ultracentrifugation in the presence of 25 mM $MgCl_2$, producing the Mg-salt form as confirmed by atomic absorption spectroscopy measurements. The content of Na, Mg, and Ca ions per 1 mg of LPS was 0.52, 25.67, and 0.87 μg, respectively. Alternatively, the concentrations can be expressed in molar ratios (mol ion/mol LPS) to better quantify the H^+ exchange in the final dialysis step. Using an LPS molecular weight of 10 400 g/mol (result of Kdo content determination), we obtain ratios of 0.24, 10.99, and 0.23 for Na, Mg, and Ca ions, respectively. Na^+-LPS was obtained through a series of dialyzation steps carried out in the following sequence: twice against 20 mM Na_2EDTA (0.5 mM HEPES, pH 8.0), twice against 20 mM Na_2EDTA and 100 mM NaCl (0.5 mM HEPES, pH 8.0), twice against 100 mM NaCl (5 mM HEPES, pH 8.0), twice against 100 mM NaCl, and five times against nanopure water. Atomic absorption spectroscopy showed 25.50, 0.43, and 1.51 μg of Na, Mg, and Ca ions per 1 mg of LPS (11.53, 0.18, 0.39 mol/mol), respectively. Finally, the LPS was converted to its Ca-salt form by dissolving the isolated Mg-salt form in 50 mM Na_4EDTA (dissolved in 10 mM Tris, pH 8.0) and, after an hour of stirring, setting the $CaCl_2$ concentration to 250 mM. The sample was then mixed with 2 volumes of ethanol and cooled to 0 °C. LPS was collected by centrifugation (15 000*g*, 18 min, 4 °C), dissolved in water, and extensively dialyzed against nanopure water. The atomic absorption spectroscopy measurement of this sample revealed 0.93 μg of Na, 0.30 μg

of Mg, and 26.34 μg of Ca ions per 1 mg of LPS (0.42, 0.13, 6.83 mol/mol, respectively). LPS's average molecular weight was calculated as 10 400 g/mol, based on Kdo content determination, and samples were assessed for DNA, RNA, and protein contamination. Sugar composition analysis was performed using the alditol−acetate method.[23] The method was used to estimate the ratios of characteristic sugars and to determine the presence of genetic materials. According to the data, samples did not contain detectable genetic materials. The LPS was further assessed for banding pattern (SDS−PAGE), lipid A molecular weight (MALDI-TOF mass spectroscopy), and polysaccharide structure (NMR spectroscopy). These experiments confirmed the integrity of the LPS samples.

Oriented Multilamellar Samples. Self-assembled, aligned LPS multibilayers with the appropriate counterion (i.e., Na^+, Ca^{2+}, or Mg^{2+}) were fabricated on substrates of single-crystal silicon. The alignment of the self-assembled bilayers was ameliorated through mechanical shearing, followed by temperature cycling between 10 and 60 °C. Routinely, the best-aligned samples were Na^+-LPS, whereas Mg^{2+}- and Ca^{2+}-LPS proved to be more problematic.

Neutron Diffraction. Neutron diffraction experiments were performed using the N5 triple-axis spectrometer located at the National Research Universal (NRU) reactor (Chalk River Laboratories, Canada). A pyrolytic-graphite (PG) monochromator was used to select 2.37 Å neutrons, while a PG filter was used to eliminate higher order reflections (i.e., $\lambda/2$, $\lambda/3$, etc.). LPS samples were placed in an airtight relative humidity sample cell[24] and hydrated to the requisite relative humidity (RH) using a series of D_2O/H_2O mixtures (i.e., 100%, 50%, and 0% D_2O). RH was controlled by saturating the various D_2O/H_2O solutions with KCl (81% RH), at a temperature of 50 °C. At this RH and temperature, LPS forms a lamellar phase.[14] The stability of the experimental conditions over the data collection period was confirmed by the reproducibility of the diffraction data, whereby the lamellar repeat spacing and the various peak intensities remained unaltered over the duration of the experiment indicating that the bilayer structure was unchanged. Typically, each experimental condition was repeated a total of three times.

The alignment quality for each sample was assessed from the Gaussian width of rocking curves (i.e., sample rotated at a fixed detector angle). For Na^+- and Ca^{2+}-LPS bilayers there is a sharp peak (mosaic spread of Gaussian width 0.06°) corresponding to the orientation of the multibilayers nearest to the Si substrate, which sits on top of a broad peak (mosaic spread of Gaussian width ~2°) corresponding to the orientation of bulk multibilayers.[25] In the case of Mg^{2+}-LPS multibilayers these mosaic spreads are 0.6° and ~4°, respectively. The diffraction peaks were fitted to Gaussians with an additional second polynomial function describing the background. Integrated intensities for the different Bragg maxima were corrected for incident flux on the sample, sample absorption, and Lorentz correction, according to well-established procedures,[26] whereas standard deviations were estimated from the fitting results in accordance to the propagation of statistical errors. 1D SLD profiles were reconstructed using the Fourier transform where the phases were determined from H_2O/D_2O contrast variation experiments.[27] To determine the crystallographic phases, three different contrast conditions (i.e., 0%, 50%, and 100% D_2O) were performed.

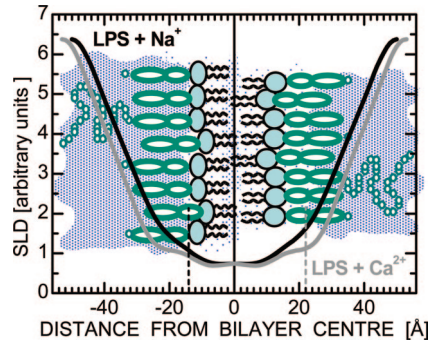

Figure 2. Arbitrary scale 1D SLD profiles obtained from the Fourier reconstruction of diffraction data from oriented LPS bilayers hydrated in 100% D_2O. The solid black line corresponds to Na^+-LPS bilayers (calculated from structure factors shown in Table 1), whereas the solid grey line corresponds to Ca^{2+}-LPS bilayers (structure factors in Table 2). The dashed lines demarcate the borders of regions that are highly accessible to water.

Results

Features in the 1D SLD profile (Figure 2) can be associated with identifiable LPS chemical moieties. The bilayer is formed by two LPS monolayers, with their hydrophilic polysaccharide chains residing in the interlayer water region, which in the 100% D_2O case has the highest SLD. From the water region, the SLD decreases in a continuous fashion to the bilayer center. The central bilayer region is made up of lipid A hydrocarbon chains, which are calculated to extend about 12.5 Å on either side of the bilayer center.[14] In contrast to commonly studied lipids (e.g., PC, PE, PG, etc.), the "central trough" typically attributed to disordered CH_3 groups,[28] seems to be less pronounced in LPS bilayers.[14] This is partly the result of D_2O in the middle of the bilayer,[14] but can also be associated to increased hydrocarbon chain order as a result of, for example partial chain interdigitation. This increased order in the LPS's bilayer center may also contribute to stabilizing the bilayer structure of these amphiphilic molecules with large hydrophilic groups.

The hydrocarbon chains are attached to the lipid A headgroup and the inner core, further extending the LPS molecule (from 12 to 24 Å on either side of the bilayer). The SLD profile is slightly higher in this region as it contains chemical groups with high neutron SLDs (e.g., phosphates and carboxylates). The SLD region associated with these groups is much more distinct in the case of Ca^{2+}-LPS bilayers, whereas in the case of Na^+-LPS bilayers this region is somewhat obscured by the presence of high-SLD D_2O. Further increases to the SLD profile reflect the ever-increasing amounts of D_2O into the outer core and O-side chain regions.

Consistent with previous results,[14] the repeat spacing of smooth Na^+-LPS multibilayers is 100 Å (106 Å in the case of Ca^{2+}-LPS), which was determined from the linear plot of the scattering vector versus diffraction peak order. Although these fits were typically resolved within a statistical error of only 0.5 Å, the variation among the different measurements resulted in a standard deviation of 3 Å. It should be mentioned that the measured repeat spacings are much greater than those previously reported for rough LPS bilayers.[29]

For the most part, the SLD profiles of Ca^{2+}- and Na^+-LPS exhibit the same structural features (Figure 2). Nevertheless, where they differ is in the outer/inner core region. Compared to Na^+-LPS, the amount of water penetrating the outer/inner core region of Ca^{2+}-LPS bilayers is substantially less. It is, however, important to note that, as a result of different scaling factors associated with the two SLD profiles, they cannot be

TABLE 1: Corrected Structure Factors of Na^+-LPS Bilayers Measured at 50 °C and 81% RH

	diffraction peak order					
D_2O content (%)	1	2	3	4	5	6
100	−106 ± 1	29.5 ± 0.4	−6.63 ± 0.17	1.90 ± 0.23	−1.69 ± 0.12	−2.09 ± 0.38
50	−48.3 ± 0.5	19.9 ± 0.1	−4.58 ± 0.19	0	−1.93 ± 0.20	1.51 ± 0.20
0	9.13 ± 0.57	−10.2 ± 0.1	2.45 ± 0.17	−1.27 ± 0.16	0	0.62 ± 0.22

TABLE 2: Corrected Structure Factors of Ca^{2+}-LPS Bilayers Measured at 50 °C and 81% RH

	diffraction peak order					
D_2O content (%)	1	2	3	4	5	6
100	−36.4 ± 1.2	13.7 ± 0.2	−3.20 ± 0.18	0	0	1.29 ± 0.43
50	−24.4 ± 0.8	9.84 ± 0.22	−2.29 ± 0.28	0	0	0
0	8.88 ± 1.52	−7.31 ± 0.33	1.47 ± 0.37	0	0	0

compared directly. The differences in hydration between the two bilayers are better appreciated by referring to the water distribution profiles shown in Figure 3.

Since the SLD of water changes in sign as a function of the D_2O/H_2O ratio, neutron scattering is an ideal technique for estimating water distribution across bilayers. The water distribution was determined from subtracting 0% D_2O SLD profiles (data not shown) from those at 100% D_2O (Figure 2)—the SLD profiles for these contrast conditions were calculated from structure factors reported in Tables 1 and 2. Although the SLD profiles for the two samples (e.g., Na^+- and Ca^{2+}-LPS) have different scaling factors, changing the contrast of a given sample (e.g., Na^+-LPS) yields SLD profiles of the same relative scale. Thus, the resultant difference profile for that sample corresponds to a normalized probability distribution of water molecules across the unit cell. It should be noted, however, that the difference profiles for the different samples (e.g., Na^+- and Ca^{2+}-LPS) may be shifted relative to each other, as their scaling depends on the amount of water in the bilayers. The subtraction of relative SLD profiles (as opposed to SLDs on an absolute scale) thus only yields a qualitative description from which we are unable to quantify the amount of water. In the region ±14 Å from the bilayer center, water molecules are seemingly distributed similarly in both Ca^{2+}- and Na^+-LPS bilayers but differ outside of this region. In the case of Na^+-LPS bilayers the amount of water begins to increase at approximately ±14 Å (inset to Figure 3), whereas this increase is not seen until approximately ±22 Å (inset to Figure 3) in Ca^{2+}-LPS bilayers, indicating that the outer/inner core region of Ca^{2+}-LPS is substantially less hydrated. Interestingly, although the amount of water differs in the two systems, the shape of the water distribution functions are fundamentally similar, implying that the O-side chains are similarly hydrated.

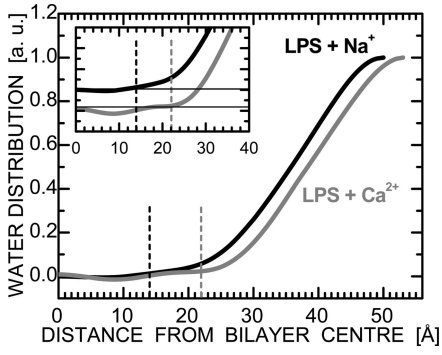

Figure 3. Water distribution profiles of Na^+- and Ca^{2+}-LPS bilayers (only half of the bilayer is shown). The water distribution functions in the O-side chain region are similar for the two systems, whereas they differ in the bilayer core. The amount of water begins to increase at ~14 Å in Na^+-LPS, whereas this increase is not seen until ~22 Å in the case of Ca^{2+}-LPS bilayers, as emphasized in the inset (vertical offset was introduced for clarity purposes).

TABLE 3: Corrected Structure Factors of Mg^{2+}-LPS Bilayers Measured at 50 °C and 81% RH

	diffraction peak order		
D_2O content (%)	1	2	3
100	−62.2 ± 3.9	19.9 ± 0.2	−6.64 ± 0.18

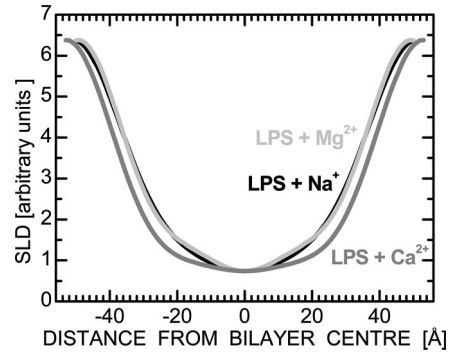

Figure 4. 1D SLD profiles calculated for oriented multilayers of Na^+-, Mg^{2+}-, and Ca^{2+}-LPS bilayers hydrated with 100% D_2O. All profiles were reconstructed using three Bragg reflections, instead of the six listed in Tables 1 and 2. The structure factors for the Mg^{2+}-LPS bilayers hydrated with 100% D_2O are reported in Table 3.

In addition to Ca^{2+}- and Na^+-LPS bilayers, we studied the effect of Mg^{2+} on LPS. Unfortunately, the Mg^{2+}-LPS bilayers yielded lower resolution diffraction patterns (only three Bragg reflections for 100% D_2O as shown in Table 3) and as a consequence, less detailed 1D SLD profiles. Figure 4 compares the 1D SLD profiles for the three different systems reconstructed using only three Bragg reflections, thus ensuring a direct comparison between the various bilayers. Interestingly, there is little difference between the Na^+- and Mg^{2+}-LPS bilayers, implying that these two counterions have a similar effect on LPS, despite their different valence number.

Discussion

There have been many studies on LPS in an attempt to establish its structure and function in bacterial membranes,[18] nearly all of which have concentrated on rough LPS.[1,2,17,19–21] Recently, neutron diffraction studies of smooth, liquid-crystalline Na^+-LPS bilayers concluded that water could penetrate into the hydrocarbon region, up to and including their bilayer center.[14]

Physiologically, Gram-negative bacteria exist in salt conditions where the predominant monovalent ion species found

associated with the OM are K^+ and Na^+ cations, whereas the divalent species are Ca^{2+} and Mg^{2+}.[8,9] Importantly, these cations are thought to play a number of significant physicochemical roles in the molecular organization of the OM. On the basis of this, it was natural to extend our previous studies to include the divalent Mg^{2+} and Ca^{2+} cations.

LPS isolated from *P. aeruginosa* PAO1 possesses a large number of negative charges. The lipid A part contains two phosphate groups, at least two more negative charges are found in the adjacent Kdo moiety, and there are three phosphate groups attached to the first heptose unit of the inner core. The semirough LPS population and B-band polysaccharide chain represent further negative charges—B-band repeat unit contains two mannuronic acid derivatives. As such, it is easy to see the relevance of cation type and concentration on LPS bilayer structure. It has been shown[19,20] that cations bind primarily to the inner core region of rough LPS mutants and also, in the case of PAO1, the inner core—lipid A region most likely represents the portion of the LPS involved in binding cations and metals.[11] In the case of Ca^{2+} cations, the LPS polar headgroup region became dehydrated and acyl chain order was found to increase. This was inferred from the decrease in the lamellar repeat spacing using X-ray diffraction, and a constant electron density of fatty acids, indicative of a more ordered acyl chain region.[20] The present results provide direct evidence for LPS dehydration by Ca^{2+} cations. In combination with the increase in lamellar repeat spacing, compared to Na^+- and Mg^{2+}-LPS bilayers, we therefore infer Ca^{2+}-LPS bilayers to be more ordered. Moreover, our results support the correlation between increased biological activity and increased levels of hydration,[20] the more active Na^+-LPS being more hydrated than the lesser active, less hydrated, Ca^{2+}-LPS (Figure 3).

In comparison to Na^+- and Mg^{2+}-LPS bilayers, the present data clearly show that water does not penetrate extensively the outer/inner core region of Ca^{2+}-LPS membranes. On the other hand, the LPS outer core and O-side specific chain regions do not seem to be affected by the different ions, judging from the slopes in the water region of the three SLD profiles (Figure 4). Although this may at first seem surprising, in view of the negative charges borne on B-band LPS, similar observations and conclusions were made for other cations.[11] It therefore seems that Ca^{2+} ions penetrate all the way into the lipid A inner core interacting with the LPS's negatively charged groups. This interaction results in a more compact organization of the core region, that excludes water (Figure 2). According to this explanation, the increased order causes the outer/inner core region to stretch and possess fewer defects, inhibiting water penetration. Although the difference in total lamellar repeat spacing between Na^+- and Ca^{2+}-LPS bilayers is only 6 Å (100 $\pm$ 3 Å vs 106 $\pm$ 3 Å, respectively), suggesting that the overall bilayer structure is not dramatically affected by Ca^{2+} ions, the impact of calcium is sufficient to induce local changes in lateral packing, affecting hydration.

Seemingly, an unexpected result is the difference between Ca^{2+}- and Mg^{2+}-LPS bilayers, despite both cations being divalent. Although there are studies that have addressed their important roles with regards to LPS structure, few have compared their effects.[18–20] In general, and compared to natural or monovalent cation salt forms, divalent cation salt forms of LPS bilayers exhibited considerable changes in physicochemical parameters. However, it was also pointed out that Ca^{2+}-LPS is orders of magnitude less active than Mg^{2+}-LPS.[20] Additionally, Mg^{2+} ions may induce local instabilities within the membrane which are not present in the case of Ca^{2+}-LPS bilayers.[18] Indirectly, this observation is in agreement with the present results where Ca^{2+}-LPS bilayers do not permit water to penetrate to the same extent as Mg^{2+}-LPS bilayers.

The differences between the hydration properties of Ca^{2+}- and Mg^{2+}-LPS bilayers may also be rationalized by the physical differences between the two cations, as identified by Sharma and Stevens.[30] First, calcium ions have a larger ionic, or Pauling radius (0.99 Å), than magnesium ions (0.65 Å). Second, the preferred coordination number for hydrated calcium ions is at least 6 (8 under crystalline conditions), and 6 for magnesium ions. Third, as a consequence of their larger crystal radius, calcium ions, compared to magnesium ions, exhibit a lower hydration energy requiring smaller amounts of energy for the removal of their hydration shells. As a result of these characteristics, calcium will preferentially bind to phosphate, carboxylate, or sulfonate groups, whereas these binding sites may not lend themselves to magnesium.[30] This is again in agreement with our results, whereby calcium cations are seen to induce structural changes in the phosphate and carboxylate-rich regions.

In conclusion, it seems that Ca^{2+} alters the structure of smooth LPS bilayers in such a manner that water does not penetrate the outer/inner core to the same extent as it does in Na^+- and Mg^{2+}-LPS bilayers. We propose that this difference in water penetration is the result of calcium "compacting" the LPS molecules in this region. In agreement with previously published data, and the chemical composition of LPS, we believe that the most likely origin of this structural rearrangement is the result of electrostatic interactions. Importantly, the peculiar response of LPS bilayers to ionic conditions together with bilayer destabilization, when subjected to elevated hydration conditions, strongly suggest a possible relation between levels of hydration and the formation of nonlamellar structures. Studies are presently underway to determine whether or not Ca^{2+}-LPS bilayers, compared to Na^+- and Mg^{2+}-LPS, are less likely to form nonlamellar phases.

Acknowledgment. This work was supported by funds through the Advanced Foods and Materials Network−Networks of Centres of Excellence (AFMnet−NCE).

References and Notes

(1) Nikaido, H. *Microbiol. Mol. Biol. Rev.* **2003**, *67*, 593–656.
(2) Wilkinson, S. G. *Prog. Lipid Res.* **1996**, *35*, 283–343.
(3) Duong, F.; Eichler, J.; Price, A.; Leonard, M. R.; Wickner, W. *Cell* **1997**, *91*, 567–573.
(4) Rocchetta, H. L.; Burrows, L. L.; Lam, J. S. *Microbiol. Mol. Biol. Rev.* **1999**, *63*, 523–553.
(5) Caroff, M.; Karibian, D. *Carbohydr. Res.* **2003**, *338*, 2431–2447.
(6) Touhami, A.; Jericho, M. H.; Boyd, J. M.; Beveridge, T. J. *J. Bacteriol.* **2006**, *188*, 370–377.
(7) Raetz, C. R.; Whitfield, C. *Annu. Rev. Biochem.* **2002**, *71*, 635–700.
(8) Baron, E. J.; Finegold, S. M. In *Bailey & Scott's Diagnostic Microbiology*, 8th ed.; The C. V. Mosby Company: St. Louis, MO, 1990.
(9) Murray, P. R.; Baron, E. J.; Pfaller, A. A.; Tenover, F. C.; Yolken, R. H. In *Manual of Clinical Microbiology*, 6th ed.; American Society for Microbiology: Washington, DC, 1995.
(10) Kadurugamuwa, J. L.; Lam, J. S.; Beveridge, T. J. *Antimicrob. Agents Chemother.* **1993**, *37*, 715–721.
(11) Langley, S.; Beveridge, T. J. *Appl. Environ. Microbiol.* **1999**, *65*, 489–498.
(12) Sadovskaya, I.; Brisson, J. R.; Thibault, P.; Richards, J. C.; Lam, J. S.; Altman, E. *Eur. J. Biochem.* **2000**, *267*, 1640–1650.
(13) Seydel, U.; Koch, M. H.; Brandenburg, K. *J. Struct. Biol.* **1993**, *110*, 232–243.
(14) Abraham, T.; Schooling, S. R.; Nieh, M. P.; Kučerka, N.; Beveridge, T. J.; Katsaras, J. *J. Phys. Chem. B* **2007**, *111*, 2477–2483.
(15) Rittig, M. G.; Kaufmann, A.; Robins, A.; Shaw, B.; Sprenger, H.; Gemsa, D.; Foulongne, V.; Rouot, B.; Dornand, J. *J. Leukocyte Biol.* **2003**, *74*, 1045–1055.
(16) Hancock, R. E. *Annu. Rev. Microbiol.* **1984**, *38*, 237–264.

(17) Naumann, D.; Schultz, C.; Sabisch, A.; Kastowsky, M.; Labischinski, H. *J. Mol. Struct.* **1989**, *214*, 213–246.
(18) Ferris, F. G.; Beveridge, T. J. *Can. J. Microbiol.* **1986**, *32*, 52–55.
(19) Snyder, S.; Kim, D.; McIntosh, T. J. *Biochemistry* **1999**, *38*, 10758–10767.
(20) Garidel, P.; Rappolt, M.; Schromm, A. B.; Howe, J.; Lohner, K.; Andra, J.; Koch, M. H.; Brandenburg, K. *Biochim. Biophys. Acta* **2005**, *1715*, 122–131.
(21) Schromm, A. B.; Brandenburg, K.; Loppnow, H.; Moran, A. P.; Koch, M. H.; Rietschel, E. T.; Seydel, U. *Eur. J. Biochem.* **2000**, *267*, 2008–2013.
(22) Darveau, R. P.; Hancock, R. E. *J. Bacteriol.* **1983**, *155*, 831–838.
(23) Sawardeker, J. S.; Sloneker, J. H.; Jeanes, A. *Anal. Chem.* **1965**, *37*, 1602–1604.
(24) Katsaras, J.; Watson, M. J. *Rev. Sci. Instrum.* **2000**, *71*, 1737–1739.
(25) Als-Nielsen, J.; McMorrow, D. In *Elements of Modern X-Ray Physics*; John Wiley & Sons, Ltd., 2001.
(26) Harroun, T. A.; Katsaras, J.; Wassall, S. R. *Biochemistry* **2006**, *45*, 1227–1233.
(27) Worcester, D. L.; Franks, N. P. *J. Mol. Biol.* **1976**, *100*, 359–378.
(28) Zaccai, G.; Blasie, J. K.; Schoenborn, B. P. *Proc. Natl. Acad. Sci. U.S.A* **1975**, *72*, 376–380.
(29) Tong, J.; McIntosh, T. J. *Biophys. J.* **2004**, *86*, 3759–3771.
(30) Sharma, G.; Stevens, C. F. *Proc. Natl. Acad. Sci. U.S.A* **1996**, *93*, 14170–14175.

JP8027963